Proceedings of the 16th International Conference on Soil Mechanics and Geotechnical Engineering

doi:10.3233/978-1-61499-656-9-459

Effects of initial static shear stress and principal stress reversal on cyclic and post-cyclic undrained shear of sand

L'influence du cisaillement statique initiale et de la rotation des contraintes principales sur le cisaillement non drainé cyclique et post cyclique du sable

K. Yasuhara, S. Murakami & H. Komine
Dept. of Urban and Civil Eng., Ibaraki University, Hitachi, Ibaraki, Japan
T. Unno
Dept. of Civil Eng., Graduate School of Tohoku University, Sendai, Miyagi, Japan

ABSTRACT
This study describes the influences of initial static shear stress (ISSS) and principal stress reversal on cyclic and post-cyclic deformation characteristics in triaxial compression and extension tests on medium-loose Toyoura sand. Results from post-cyclic monotonic triaxial tests on specimens with and without ISSS showed that that the post-cyclic stiffness of anisotropically consolidated specimens with an ISSS increased in compression, but decreased in the case of post-cyclic extension loading. On the other hand, the post-cyclic stiffness of specimens subjected to ISSS in the extension domain decreased during cyclic loading in compression and increased in extension.

RÉSUMÉ
Cette étude décrit l'influence de la rotation des contraintes principales sur les caractéristiques du déformations cycliques et post-cycliques au cours des essais de compression et d'extension triaxial sur le sable de Toyoura moyennement lâche. Les résultats des essais monotones post-cycliques sur des échantillons avec et sans ISSS a montrée que la rigidité des échantillons anisotropiquement consolidés a augmenté dans le cas de compression et diminué dans celui d'extension. D'autre part, la rigidité post-cyclique des échantillons subissant le ISSS décroit lors du chargement cyclique en compression et augmente en extension.

1 INTRODUCTION

Saturated soils suffer from deformation and settlement that results from degradation of both stiffness and strength. Cyclic or transient loading triggers that degradation. Elucidating the mechanisms of these phenomena is useful for investigating sequential behaviour during cyclic and subsequent post-cyclic loading of soils. This purpose can be accomplished by following the procedure of cyclic laboratory tests that was proposed by the authors (Yasuhara et al., 1992; Yasuhara and Nagano, 1995; Yasuhara and Hyde, 2002), as shown in Fig. 1. This is commonly available in cyclic triaxial and cyclic-DSS or direct shear tests (Yasuhara et al., 1992; Yasuhara and Nagano, 1995) not only on non-plastic soils and sandy soils, but also on plastic soils and cohesive soils. The first half of this presentation highlights the results of an investigation of cyclic and post-cyclic behaviour of sand. This study specifically addresses post-cyclic behaviour of sand with special reference to effects of initial static shear stress (ISSS).

2 CYCLIC AND POST-CYCLIC TRIAXIAL TESTS ON SAND

2.1 *Cyclic and post-cyclic triaxial tests*

The cyclic triaxial test that is used herein was proposed previously by the authors (Yasuhara et al., 1992; Yasuhara and Nagano, 1995). It has been adopted mainly for fine-grained soils. It includes procedures for stress-controlled cyclic triaxial tests and subsequent strain-controlled monotonic triaxial tests.

2.2 *Testing procedure*

Toyoura sand was used in all triaxial tests in which each specimen with 50% of the average relative density with 5 cm diameter and height. Samples were prepared using air-pluviation method. Confining pressure for isotropic consolidation prior to undrained cyclic loading was 98 kPa with a sustained period of 1 h. To investigate effects of initial static shear stress (ISSS) and principal stress reversal on cyclic and post cyclic stiffness degradation behaviour, the same kinds of tests on specimens with $q_s/p'_c = 0.75$ in the compression domain and with $q_s/p'_c = -0.51$ in the extension domain, both under p'_c = 98 kPa were also conducted. In those tests, qs is the initial deviatoric stress equal to $\sigma'_{ao}-\sigma'_{ro}$, where σ'_{ao} is the effective axial stress and σ'_{ro} is the effective radial stress, repectively, before cyclic loading. In these cases, the same confining pressure, p'_c = 98 kPa, as that for

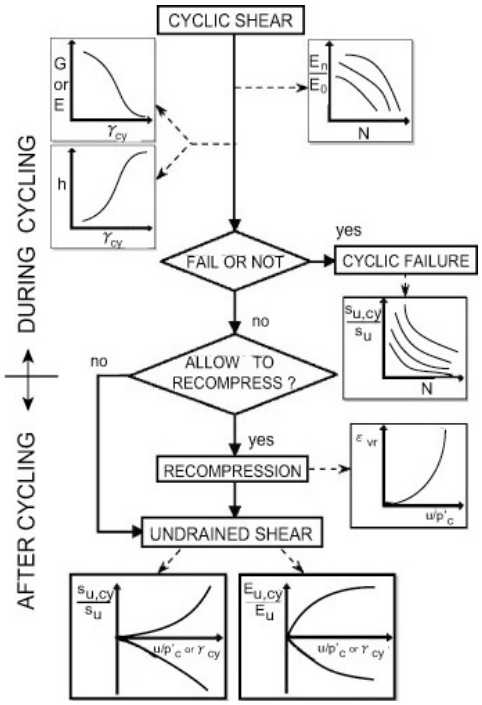

Figure 1. Schematic diagram for the procedure of cyclic and post-cyclic shearing tests

isotropic consolidation without ISSS was attained by step-drained shear loading. Cyclic triaxial tests were carried out to combine the number of load cycles, N, and the cyclic shear stress level, $(q_{cyc})/2/p'_c$. The normalized excess pore pressures, $\Delta u/p'_c$, generated by undrained cyclic loading were selected as a parameter to indicate the magnitude of cyclic loading history.

3 CYCLIC BEHAVIOUR

Both Fig. 2 and Fig. 3 illustrate a set of effective stress paths and stress vs. strain relations of specimens with and without ISSS during undrained cyclic loading. Furthermore, post-cyclic undrained monotonic results are also depicted in Fig. 4 and Fig. 5, respectively, for specimens with and without ISSS. The specimens with ISSS tend to exhibit residual deformation toward the direction of ISSS (compression or extension). The more shear stress is skewed towards the extension domain, the more marked the absolute magnitude of its deformation. However, neither specimen becomes liquefied. The cyclic-induced excess pore pressures are not so pronounced ($\Delta u/p'_c$ = 0.35). On the other hand, specimens without ISSS are liquefied and shear strains are dragged toward the extension region. In light of this fact, we infer that residual shear strains during undrained cyclic shear loading become noticeable in cases in which cyclic loading is applied on the extension side. In addition, sand specimens are easily liquefied when undergoing principal stress reversal. This trend is similar to that of post-cyclic monotonic shear behaviour, as will be explained later.

4 POST-CYCLIC BEHAVIOUR

In addition to behaviour during cyclic loading, we investigated post-cyclic behaviour with a special emphasis on effects of ISSS and principal stress rotation. Three specimens were started from states in p'-q spaces with and without ISSS. The ISSS was applied in both domains of compression and extension. The effective stress path in p'-q spaces and stress-strain relations in monotonic loading after cyclic loading are summarized in Fig. 4 and Fig. 5, respectively. The symbols ○ and ● in both figures show the respective starting points for monotonic loading tests on specimens with and without ISSS. $\Delta u/\sigma'_c$ and ε_{cyc} are excess pore pressure normalized by confining pressure and residual axial strain after cyclic loading, respectively.

4.1 Investigation of post-cyclic effective stress path

Fig. 4 indicates that:

i) the decrease in the mean effective principal stress is less marked in the specimen for (a) series with ISSS in the compression side. Even when p' decreases, it recovers rapidly; therefore, the specimen must dilate. On the other hand, in post-cyclic extension shear, the effective stress path reaches the origin of p'-q spaces. Thereafter, it crawls along the CSL, showing dilatancy, even when the excess pore pressure ratio is as small as $\Delta u/\sigma'_c = 0.4$.

ii) post-cyclic compression shear behaviour for specimens of test series (b), which follows principal stress rotation during cyclic loading, demonstrates the behaviour of quasi-overconsolidated specimens similarly to those undergoing ISSS in the compression domain. Specimens become softened during post-cyclic extension shear and then tend to dilate.

iii) Unique behaviour is observed in post-cyclic compression and extension tests on specimens with ISSS in the extension domain. (a) The specimen is liquefied. Then, under post-cyclic monotonic compression loading, it tends to dilate. (b) Similarly, post-cyclic extension shear produces dilatation even if the cyclic-induced excess pore pressures are small.

4.2 Post-cyclic stress and strain relations

1) Fig. 5(a) shows post-cyclic stress-strain curves of the specimen with ISSS in the compression domain. The specimen underwent no principal stress rotation during cyclic loading. It shows a hardening tendency in comparison with that with no cyclic loading, which becomes softer with increasing $\Delta u/p'_c$ during cyclic loading. In contrast, the compressive stress vs. strain curve of the specimen shows a

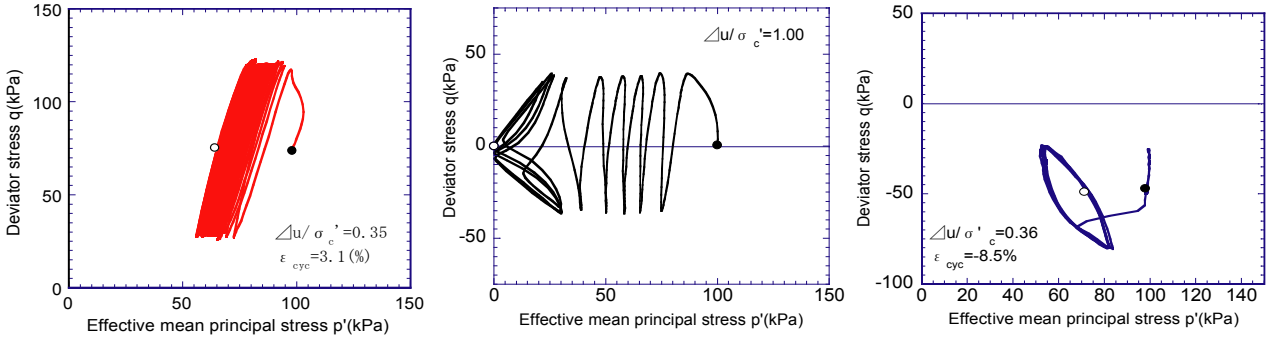

(a) ISSS-Compression, (b) isotropic consolidation, (c) ISSS-Extension
Figure 2. Effective stress path during cyclic loading

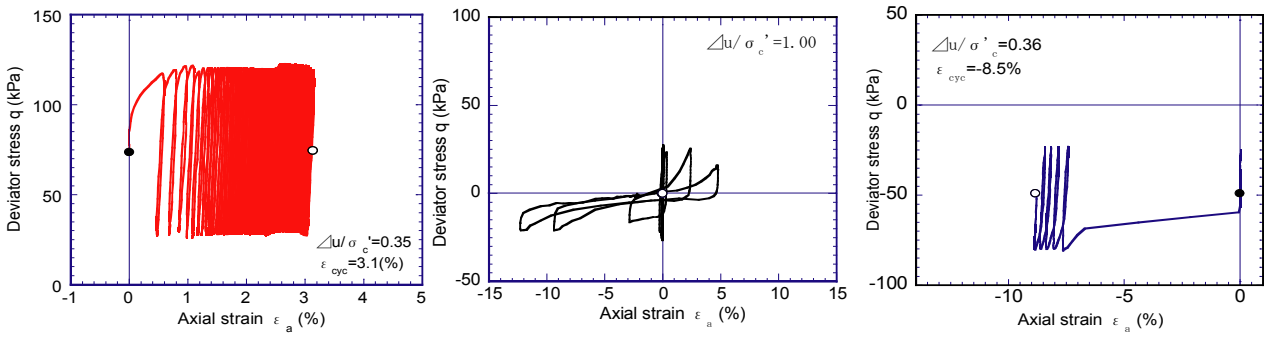

(a) ISSS-Compression, (b) isotropic consolidation, (c) ISSS-Extension
Figure 3. Stress vs. strain relations during cyclic loading

hardening tendency.

2) Post-cyclic stress and strain curves of isotropically consolidated specimens with no ISSS from both compression and extension tests become softened. Strength decreases with increasing $\Delta u/\sigma'_c$. This fact reflects stress reversal during cyclic loading.
3) Comparison of post-cyclic compressive stress vs. strain curves of specimens subjected to cyclic loading under ISSS in the extension domain with those both with ISSS in the compression domain and with no ISSS. No recovery of deviatoric stress occurs until application of a large compressive strain (10% in this case), as shown in Fig. 5(c), even in the case where the cyclic-induced pore pressure ratio, $\Delta u/\sigma'_c$, is as small as 0.35. Stress reversal during cyclic loading markedly reduces the undrained compression strength of sand.
4) An unprecedented aspect of stress-strain curves is shown in Fig. 5(c). That figure presents results of post-cyclic extension tests on a specimen undergoing undrained cyclic loading only in the extension domain. These results indicate that the shear resistance of the specimen recovers with ISSS in the extension, thereby engendering hardening, even though the specimen is subjected to extensional cyclic loading.
5) When synthesizing the finding indicated in item (4), and the shear behaviour of a specimen undergoing undrained cyclic loading only in the compression domain as shown in Fig. 5(a), undrained cyclic loading produces hardening in specimens when the direction of post-cyclic monotonic shearing stress application, whether compression or extension, is the same as that during undrained cyclic loading.
6) On the other hand, the opposite tendency is observed when the direction of post-cyclic loading differs from that of undrained cyclic loading. Shear resistance decreases when a specimen is subjected to post-cyclic monotonic loading in the opposite direction from undrained cyclic loading. Post-cyclic monotonic loading may sometimes engender liquefaction even under the small decrement in effective stress. Cyclic loading inclined either in compression or extension produces stress induced anisotropy in soil particle structures, which subsequently engenders a higher shear resistance in the case where post-cyclic monotonic loads are applied in the direction of cyclic loading, and a lower shear resistance in the opposite case.

5 QUANTITATIVE REPRESENTATION OF STIFFNESS DEGRADATION

The normalized cyclic-induced excess pore pressure (EPWPR), $\Delta u/p'_c$, was selected as the parameter that describes degradation characteristics of medium dense sand subjected to undrained cyclic loading. This interpretation specifically addressed results from post-cyclic monotonic compression and extension loading on isotropically consolidated sand. Degradation in the secant modulus was determined by deviatoric stress corresponding to 0.1% axial strain in stress and strain curves, as shown in Figs. 6(a) and 6(b), by following the procedure adopted in the previous study (Nagase et al., 1997). Almost the same cyclic stress ratio, $q_{cyc}/2p'_c$, equal to 0.129 in Fig. 6(a) and to 0.132 in Fig. 6(b), was employed for post-cyclic compression and extension tests, respectively. Results in both figures show that the absolute value of recoverable strain, ε_r, in the shear resistance force in extension shear is larger than that in compression shear. This value of ε_r is in accordance with an inflection point (designated by dashed line) in which the normalized excess pore pressure recovers rapidly, as shown in Fig. 7, which contrasts $\Delta u/p'_c$ to axial strain. This fact verifies the utility of $\Delta u/p'_c$ as an important parameter.

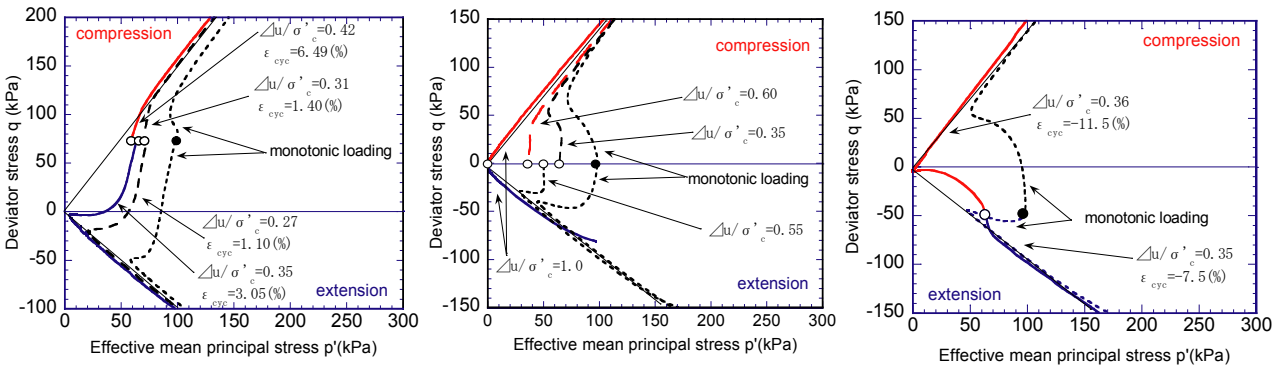

(a) ISSS-Compression, (b) isotropic consolidation, (c) ISSS-Extension
Figure 4. Effective stress path during post-cyclic monotonic loading

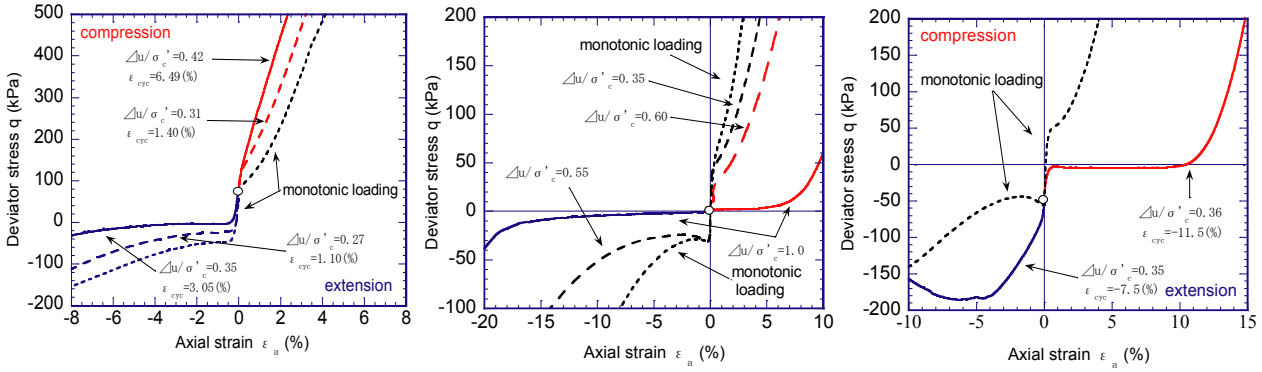

(a) ISSS-Compression, (b) isotropic consolidation, (c) ISSS-Extension
Figure 5. Stress vs. strain relations during post-cyclic monotonic loading

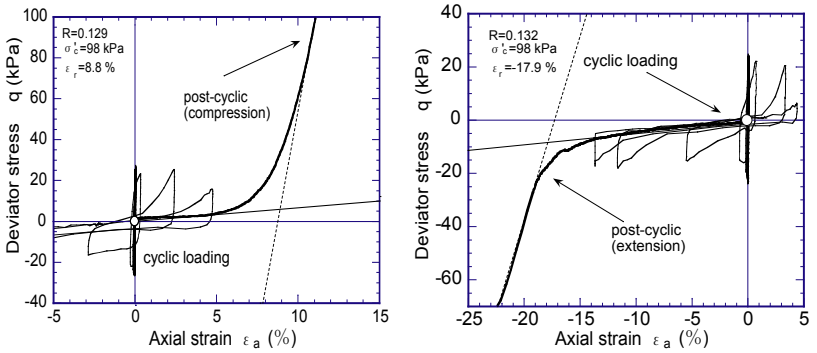

(a) Isotropic consolidation – Compression, (b) Isotropic consolidation - Extension
Figure 6. Stress vs. strain relations during cyclic and post-cyclic monotonic loading

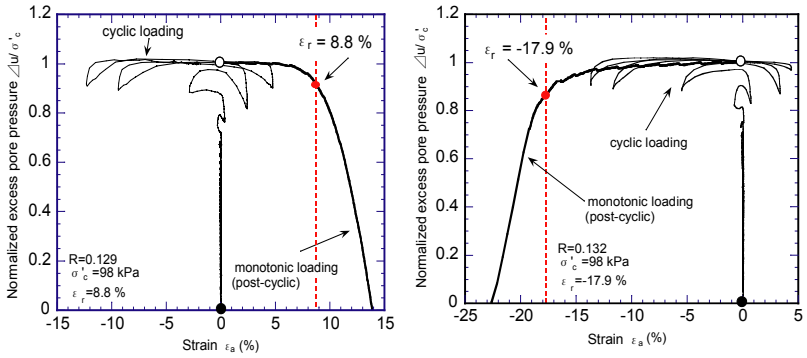

(a) Isotropic consolidation – Compression, (b) Isotropic consolidation - Extension
Figure 7. Normalized excess pore pressure vs. strain relations during cyclic and post-cyclic monotonic loading

Fig. 8 presents results in which the post-cyclic Young's modulus that was shown in Fig. 5(b) and normalized by the Young's modulus, $E_{s,cyc}$, without any cyclic loading history is plotted against $\Delta u/p'_c$. The following tendencies are shown by results from Fig. 8:

i) Plotted against $\Delta u/p'_c$, the degradation in post-cyclic stiffness ratio in extension shear is greater than that in compression shear, but no marked overall difference is apparent for either one.

ii) The stiffness ratio decrease becomes marked in the region around 0.8 of $\Delta u/p'_c$ both in post-cyclic compression and extension tests.

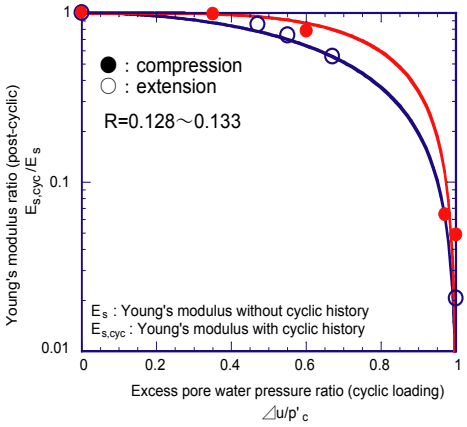

Figure 8. Young's modulus ratio vs. normalized excess pore pressure relations

6 CONCLUSION

The present paper includes effects of stress-reversal produced by ISSS on cyclic and post-cyclic shear resistance of medium loose sand in triaxial conditions.

Results from cyclic triaxial tests on specimens with and without ISSS indicate that:

1) Specimens with ISSS during the pre-compression stage do not undergo liquefaction ($\Delta u/p'_c = 1.0$), but specimens with ISSS do.

2) Shear strain occurs more markedly in a specimen undergoing cyclic loading in the extension domain than one in the compression domain. Further, principal stress reversal during cyclic loading contributes to increased cyclic shear strain. On the other hand, results from post-cyclic undrained monotonic tests indicate that:

1) Isotropically-consolidated specimens are subjected to principal stress reversal during undrained cyclic loading. Therefore, they markedly decrease stiffness in cases of post-cyclic compression and extension monotonic loading. In particular, this tendency is more eminent in post-cyclic extension tests than in compression tests. This fact indicates that principal stress reversal during cyclic loading induces stiffness softening during monotonic shearing of sand as it experiences cyclic loading.

2) Post-cyclic stiffness of anisotropically consolidated specimens with ISSS in post-cyclic monotonic triaxial tests increases stiffness in the compression domain, whereas stiffness decreases in the case of post-cyclic extension loading. Stiffness of specimens undergoing ISSS in the extension domain shows a completely different tendency. Post-cyclic stiffness of specimens with ISSS in the extension domain during cyclic loading decreases stiffness in the compression domain, but it increases stiffness in the extension domain. Therefore, it can be concluded that the specimens lose their stiffness in cases where the direction of post-cyclic undrained shear is different from the domain in which they are subjected to undrained cyclic loading. This tendency must be connected with the fact that principal stress reversal triggers destruction of stress-induced anisotropy in soil structures that are produced by application of ISSS.

3) The stiffness ratio in which the post-cyclic secant Young's modulus is normalized by the initial one before cyclic loading decreases with increasing excess pore pressure normalized by the initial mean effective principal stress. This normalization is similar with both results in post-cyclic compression and extension tests, but the stiffness decrement is slightly more marked in post-cyclic extension than that in post-cyclic compression.

REFERENCES

Nagase, H., Hiro-oka, A. and Yanagihara, T. 1997. Deformation characteristics of liquefied loose sand by triaxial compression tests, Proc. International Conf. Deformation and Progressive Failure in Geomechanics, *IS-NAGOYA'97*, Vol. 1, 559–564, Nagoya, Japan.

Yasuhara, K., Hirao, K. and Hyde, A. F. L. 1992. Effects of cyclic loading on undrained strength and compressibility of clay, *Soils and Foundations*, Vol. 32, No. 1, 100–116.

Yasuhara, K. and Hyde, A. F. L. 1997, a. Method for estimating post-cyclic undrained secant modulus of clays, *J. Geotech. & Geoenvironmental Eng*., ASCE, 123(3), 204–211.

Yasuhara, K., and Toyota, N. 1997, b. Effects of initial static shear stress on post-cyclic degradation of a plastic silt, *Proc. 14th ICSMFE*, Hamburg, Germany, Vol. 1, 439–442.

Yasuhara, K., Hyde, A. F. L. and Murakami, S. 2004. Post-cyclic degradation of saturated plastic silts, Proc. *International Symposium on Cyclic Behaviour of Soils and Liquefaction Phenomena*, Bochum, Germany, 275–286.